



HAL
open science

Geomechanics in Reservoir Simulation: Overview of Coupling Methods and Field Case Study

P. Longuemare, M. Mainguy, P. Lemonnier, A. Onaisi, C. Gérard, N. Koutsabeloulis

► **To cite this version:**

P. Longuemare, M. Mainguy, P. Lemonnier, A. Onaisi, C. Gérard, et al.. Geomechanics in Reservoir Simulation: Overview of Coupling Methods and Field Case Study. Oil & Gas Science and Technology - Revue d'IFP Energies nouvelles, 2002, 57 (5), pp.471-483. 10.2516/ogst:2002031 . hal-02043967

HAL Id: hal-02043967

<https://ifp.hal.science/hal-02043967>

Submitted on 21 Feb 2019

HAL is a multi-disciplinary open access archive for the deposit and dissemination of scientific research documents, whether they are published or not. The documents may come from teaching and research institutions in France or abroad, or from public or private research centers.

L'archive ouverte pluridisciplinaire **HAL**, est destinée au dépôt et à la diffusion de documents scientifiques de niveau recherche, publiés ou non, émanant des établissements d'enseignement et de recherche français ou étrangers, des laboratoires publics ou privés.

Geomechanics in Reservoir Simulation: Overview of Coupling Methods and Field Case Study

P. Longuemare¹, M. Mainguy¹, P. Lemonnier¹
A. Onaisi², Ch. Gérard³ and N. Koutsabeloulis⁴

¹ Institut français du pétrole, 1 et 4, avenue de Bois-Préau, 92852 Rueil-Malmaison Cedex - France

² TotalFinaElf, CSTJF, avenue Larribau, 64018 Pau Cedex - France

³ Beicip-Franlab, 232, avenue Napoléon-Bonaparte, BP 213, 92502 Rueil-Malmaison Cedex - France

⁴ VIPS (Vector International Processing Systems) Ltd - United Kingdom

e-mail: pascal.longuemare@ifp.fr - marc.mainguy@ifp.fr - patrick.lemonnier@ifp.fr
atef.onaisi@totalfinaelf.com - christophe.gerard@beicip.fr - nick.koutsabeloulis@vips.co.uk

Résumé — Géomécanique en simulation de réservoir : méthodologies de couplage et étude d'un cas de terrain

— Cette publication traite de la modélisation des effets géomécaniques induits par l'exploitation des réservoirs et de leur influence sur les écoulements de fluide dans les réservoirs. Ces effets géomécaniques peuvent être relativement conséquents dans le cas des réservoirs faiblement consolidés et des réservoirs fracturés. Les principaux mécanismes couplés intervenant lors de la production de ces réservoirs, ainsi que les méthodes permettant de les modéliser, sont présentés. Le comportement géomécanique d'un cas réel est ensuite étudié. Un simulateur couplé — ATH2VIS — est utilisé afin de quantifier les effets géomécaniques induits par l'exploitation d'un réservoir carbonaté fortement hétérogène et compartimenté. Ce simulateur met en œuvre un couplage explicite et gère les échanges de données entre le simulateur de réservoir ATHOS™ développé à l'IFP et le simulateur de géomécanique VISAGE™ (VIPS Ltd. 2001). Le résultat des simulations couplées indique que la modification de l'équilibre mécanique du milieu se traduit par une localisation de la déformation sur certaines failles en fonction de leur orientation et des variations de pression et de température dans leur voisinage. Il est également observé que seule une partie de la faille atteint le seuil de déformation plastique. Au cours de l'analyse couplée, le tenseur de déformation plastique sur les plans de faille est traduit en variation de la transmissibilité de la faille afin d'améliorer la représentation des écoulements dans le réservoir et de faciliter le calage des historiques de production.

Abstract — Geomechanics in Reservoir Simulation: Overview of Coupling Methods and Field Case Study

— The paper addresses the modeling of geomechanical effects induced by reservoir production and their influence on fluid flow in the reservoir. Geomechanical effects induced by reservoir production can be particularly pronounced in stress sensitive reservoirs, such as poorly compacted reservoirs and fractured reservoirs. The authors review the main coupled mechanisms associated with the production of these reservoirs, and describe the different approaches that can be used to solve the coupling between fluid flow and geomechanical problems. A field case study is then presented. A stress dependent reservoir simulator—ATH2VIS—was used to quantify effects associated with the production of a highly heterogeneous and compartmentalized limestone reservoir. This simulator relies on a partial coupling approach with different time steps for reservoir and geomechanical simulations and manages data exchanges at given time intervals between the ATHOS™ reservoir simulator developed at IFP and the

VISAGE™ geomechanical simulator (VIPS Ltd., 2001). The results of the coupled reservoir geomechanical simulations indicate that perturbation of the reservoir mechanical equilibrium specifically leads to progressive strain localization on a limited number of faults. Only specific parts of these faults are critically stressed, depending on pore pressure variations in their vicinity, temperature variations, and fault strikes compared with stress orientation. The normal strains resulting from geomechanical computations are interpreted in terms of permeability variations using a fracture and fault permeability model to improve the dynamic description of fluid flow and history matching.

INTRODUCTION

Variations in reservoir pressure, saturation and temperature caused by reservoir production induce changes in the stress state in and around the reservoir. Geomechanical effects can be particularly pronounced for some reservoirs, such as poorly compacted reservoirs and fractured or faulted reservoirs. In this paper, the authors first review how fluid flow and stresses are coupled, and go on to describe the main mechanisms and constitutive behaviors associated with the production of stress sensitive reservoirs. For poorly compacted reservoirs, stress changes can enhance fluid recovery due to reservoir compaction. However, reservoir compaction can also reduce reservoir permeability, cause surface subsidence and inflict damage on well equipment. These effects can only be accounted for by a highly developed geomechanical analysis that necessarily includes nonlinear elasto-plastic constitutive behavior, water weakening effects, stress path and initial stress state influences. Fractured and faulted reservoirs are generally highly compacted and thus severely affected by stress changes induced by reservoir thermal variations (cold water injection). The resulting stress changes may increase or reduce fracture conductivity and create preferred flooding directions. The modeling of faulted/fractured reservoirs therefore demands an accurate description of the hydro-mechanical constitutive behavior of joints (joint transmissivity *versus* strain relationship).

The authors then discuss different methodologies and coupling levels that can be used to solve a coupled thermo-hydro-mechanical problem. They describe the fully coupled and partially coupled approaches that can be used to solve the stress dependent reservoir problem. The fully coupled approach simultaneously solves the whole set of equations in one simulator. It yields to consistent descriptions but published works indicate that the hydraulic or geomechanical mechanisms are often simplified by comparison with conventional uncoupled geomechanical and reservoir approaches. The partially coupled approach is based on an external coupling between conventional reservoir and geomechanical simulators. This approach has the advantage of being flexible and benefits from the latest developments in physics and numerical techniques for both reservoir and geomechanical simulators. Depending on the physical mechanisms investigated, this coupling methodology can be iterated or not but in all cases, it must be designed in order to ensure a consistent and stable process.

A five-year production period of a faulted and fractured reservoir is then modeled using a 3D stress dependent reservoir simulator, with a special focus on the modeling of stress evolution during reservoir production and associated fault and fracture permeability enhancement. The ATH2VIS stress dependent reservoir simulator is based on an explicit (iterative) coupling between the *IFP* ATHOS™ reservoir simulator and the *VISAGE™* system (*VIPS Ltd., 2001*), and manages data exchanges between these simulators at preset time intervals.

The analysis indicates that during reservoir production, changes in pore pressure and temperature modify the mechanical equilibrium of the reservoir and lead to progressive strain localization on some faults. Only specific parts of these faults are critically stressed, depending on pore pressure variations in their vicinity, temperature variations, and fault strikes compared with the stress directionality. At given times of the coupled modeling, fault transmissivity variations deduced from computed strains are integrated in the reservoir simulation to improve fluid flow description and history matching.

1 GEOMECHANICAL EFFECTS INDUCED BY RESERVOIR PRODUCTION

The analysis of geomechanical effects induced by reservoir production is presented for two kinds of reservoirs, weakly consolidated reservoirs and highly compacted, fractured and faulted reservoirs.

1.1 Weakly Compacted Reservoirs

The main geomechanical effect associated with the production of weakly compacted reservoirs is reservoir compaction and the associated enhancement of fluid recovery. In the case of the Bachaquero field in Venezuela, compaction is found to be the main cause of production on half of the reservoir (*Merle et al., 1976*).

Charlez (1997) described the dominant effect of compaction drive of the recovery rate during production of the Zuata field. The author models the production of a cylindrical drainage area including steam injection at the producer. The results (*Fig. 1*) indicate significant reservoir compaction and associated pore pressure build-up that is

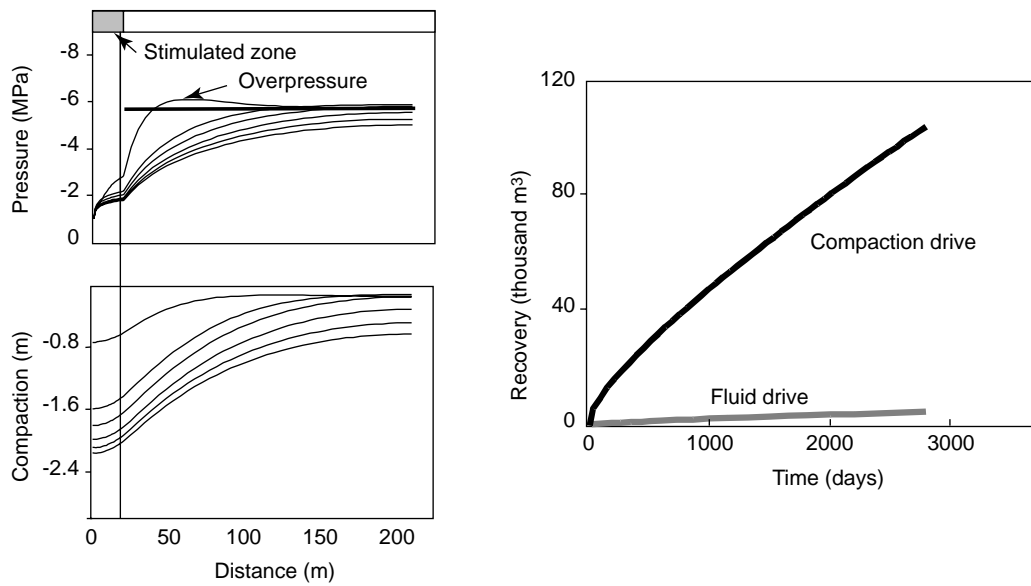


Figure 1
Zuata field case (Charlez, 1997).

observable on the pore pressure profile (stress arching effect). The results presented clearly indicate that the recovery factor is dominated by compaction drive.

Depending on overburden properties, reservoir compaction can propagate to the surface and generate subsidence. Tolerances on subsidence magnitude strongly depend on the context and field location (Boutéca *et al.*, 1996). For example, a magnitude of several meters of subsidence was damageable for the Ekofisk field (North Sea) whereas, due to high environmental constraints, the critical magnitude ranges between some centimeters to tens of centimeters for the Groningen field (Geertsma, 1989). Reservoir compaction can also reduce reservoir permeability due to high porosity reduction (Ferreira *et al.*, 1997; Wong *et al.*, 1997) and lead to well instabilities and casing collapse.

The constitutive behavior of weakly compacted reservoir rocks is nonlinear, elasto-(visco)-plastic, including pore collapse mechanism, and strongly depends on stress path and temperature. In the case of high porosity chalks, the constitutive behavior can be highly affected by water weakening mechanisms (Hermansen *et al.*, 2000; Homand, 2000; Matà, 2001).

1.2 Highly Compacted, Faulted and Fractured Reservoirs

The production of highly compacted reservoirs is associated with low reservoir compaction, and the main geomechanical effects are induced by fracturing and changes in fracture conductivity caused by thermo-poro-elastic effects (Gutierrez

and Makurat, 1997). For these reservoirs, thermo-elastic effects gradually predominate with the increase of reservoir rock mechanical stiffness. A local calculation of stress variation due to thermo-hydro-elastic effects is presented in Figure 2, assuming two reservoir rock types (low and high dolomitic content), a 100 bar pore pressure variation and a 35°C temperature variation. It clearly indicates, on one hand, that thermo-elastic effects can generate high magnitude stress variations for stiff rocks compared with variations induced by hydro-elastic effects. On the other, at field scale, thermo-elastic effects generally remain concentrated around water injectors while hydro-elastic effects affect the whole field.

Thermo-elastic effect: $\sigma_{Thermal} = E \alpha \Delta T / (1-\nu)$		
	High dolomitic content	Low dolomitic content
E	240 000 bar	120 000 bar
ν	0.2	0.2
α	2.5E-5	2.5E-5
$\alpha_{Thermal}/1^{\circ}C$	7.5 bar/ $^{\circ}C$	3.75 bar/ $^{\circ}C$
$\Delta stress (\Delta T = 35^{\circ}C)$	262 bar	131 bar

Hydro-elastic effect: $\sigma_{Hydro} = b \Delta P (1-2\nu) / (1-\nu)$	
Biot's coefficient	0.7
ν	0.2
$\alpha_{Hydro}/1bar$	0.87 bar/bar
$\Delta stress (\Delta P = 100 bar)$	87 bar

p = pore pressure, E = Young's modulus, ν = Poisson's ratio, α = thermal expansion

Figure 2
"Local" estimates of stress evolution due to pore pressure and temperature variations.

The main physical specificity of such reservoirs is the complex thermo-poro-mechanical behavior of the fractured system. The constitutive behavior depends on the density and orientation of the fracture sets, the initial stress state, and the stress path during reservoir production. Due to the high stiffness of the matrix (intact rock), the strains are localized on fracture and fault planes altering their hydraulic conductivity. Published works support some evidence of preferred flooding directions during floodwater in both naturally fractured reservoirs and unfractured reservoirs (Koutsabeloulis *et al.*, 1994; Heffer *et al.*, 1994).

2 FORMULATIONS FOR COUPLING BETWEEN FLUID FLOW AND GEOMECHANICS

2.1 Conventional Fluid Flow Formulation

In conventional fluid flow formulations, the pore volume variation only depends on the pore pressure variation through a pore volume compressibility coefficient. Assuming single phase fluid flow, the fluid mass balance formulation is expressed as:

$$\frac{k}{\eta} \nabla^2 p = \phi_0 c_{\text{fluid}} \dot{p} + \phi_0 c_{\text{rock}} \dot{p} \quad (1)$$

with:

\dot{p} = pore pressure derivative with respect to time

∇^2 = Laplacian operator

k = intrinsic permeability of the rock

η = fluid dynamic viscosity

ϕ_0 = initial porosity

c_{fluid} = fluid compressibility accounting for fluid density changes with pore pressure

c_{rock} = rock compressibility accounting for pore volume strains following pore pressure changes.

The rock compressibility assumes that the stress path followed by the reservoir is *a priori* known and constant (usual reservoir stress paths are based on uniaxial or hydrostatic strain conditions). Reservoir permeability is unaffected by pore pressure changes.

During the production of highly compacted, faulted and fractured reservoirs, strain localization on fracture and fault planes can cause a change in the permeability (or transmissibility) on the left-hand side of Equation (1). For weakly compacted reservoirs, the expected large rock deformations associated with reservoir depletion can act both on the reservoir permeability as well as the fluid accumulation term through the rock compressibility factor on the right-hand side of Equation (1). To account for geomechanical effects due to stress changes in and around the reservoir, the fluid flow problem must be solved with a geomechanical model that can correctly predict the evolution

of stress dependant parameters, such as porosity, rock compressibility, and permeability.

2.2 Formulation of Advanced Coupled Methodologies between Fluid Flow and Geomechanics

The modeling of geomechanical effects demands a rigorous integration of mechanical concepts in reservoir simulation. The coupling between reservoir simulation and geomechanics can be described by a set of two equations accounting for the deformation of the skeleton and the fluid motion in the rock porosity (see *e.g.*, Biot, 1941; Boutéca, 1992; Coussy, 1995; Lewis and Schrefler, 1998). After space-time discretization, the coupled problem can be written in the following form (Settari and Walters, 1999):

$$K \Delta_t u + L \Delta_t p = F \quad (2)$$

$$L^T \Delta_t u + E \Delta_t p = R \quad (3)$$

Equation (2) accounts for the geomechanical equilibrium whereas Equation (3) represents the fluid mass balance equation. In Equation (2), K is the stiffness matrix, u the displacement vector, L the coupling matrix between mechanical and flow unknowns (here, displacement and pore pressure) and F the vector of force boundary conditions. The coupling matrix L depends on the Biot stress coefficient. In Equation (3), L^T is the transposed matrix of L , E is the flow matrix, p the pore pressure, and R a source term for the flow problem. The decomposition $E = T - D$ is used where T is a symmetric transmissibility matrix and D is the accumulation diagonal matrix. Finally, in Equations (2) and (3), Δ_t represents the change over time so that $\Delta_t u = u^{n+1} - u^n$ and $\Delta_t p = p^{n+1} - p^n$ with n the index of time discretization. Note that, to simplify the presentation, the stiffness matrix K and the flow matrix E are considered here to be linear operators. In general, however, K and E are nonlinear operators accounting for nonlinear elasticity and nonlinear reservoir problems.

Equations (2) and (3) are coupled through the coupling matrix L . On the one hand, the pore pressure gradient affects the stress equilibrium equation through the term $L \Delta_t p$. On the other, the displacement vector acts on the flow problem by means of the $L^T \Delta_t u$ term accounting for reservoir volumetric strains. In the case of highly compacted, faulted and fractured reservoirs, the coupling may also lead to a modification of the transmissibility matrix T due to fracture and fault permeability enhancement resulting from rock deformation. For the water weakening effect, the saturation flow unknown (not included in Equations (2) and (3)) will alter the stiffness matrix K .

Settari and Walters (1999) describe the different coupling levels that can be used to solve the whole set of Equations (2) and (3).

In **conventional reservoir** simulators, the geomechanical equilibrium Equation (2) is disregarded and rock deformation is ignored so that the problem only requires the determination of the pore pressure satisfying $(T - D) \Delta_t p = R$. The latter equation appears to be the discretization of the diffusion Equation (1). According to this diffusion equation, the diagonal matrix D can account for the rock compressibility factor provided the rock deformation is known and is only pressure dependent for each cell of the reservoir mesh. This approach implicitly assumes stress changes in each block, although the stresses are not explicitly computed.

In the **partially coupled** (also called loosely coupled) approach, the stress and flow equations are solved separately (*i.e.* with two different simulators) but information is exchanged between both simulators. In terms of Equations (2) and (3), the partial coupling consists in first computing the pore pressure p assuming that the displacement vector u is known from a previous geomechanical simulation:

$$[T - D] \Delta_t p = R - L^T \Delta_t u \quad (4)$$

This computation is performed with a conventional reservoir simulator using a porosity correction depending on the displacement vector u (see Settari and Mourits, 1994, 1998). Then, using the pore pressure solution of (4), the geomechanical equilibrium equation (2) gives the displacement vector in the form:

$$K \Delta_t u = F - L \Delta_t p \quad (5)$$

The displacement vector computation is performed with a conventional stress simulator in which pressure changes can be imposed as external loads.

Different coupling levels can be achieved for the partially coupled methodology. The partial coupling is termed **explicit** if the methodology is only performed once for each time step, and **iterative** if the methodology is repeated to convergence of the stress and fluid flow unknowns. As underlined by Settari and Walters (1999), the iteratively coupled method ensures the same result as the fully coupled method.

“One way coupling” is the simplest partially coupled approach in which the pore pressure history deduced from a conventional reservoir simulation is introduced into the geomechanical equilibrium equation in order to compute the new stress equilibrium. This kind of coupling involves no mechanical effects on the reservoir simulation and the mechanical result is only used to analyze stress and strain localization for well equipment damage or environmental problems. This coupling is easy to implement and still includes some interesting physics.

In the literature, the partial coupling approach often uses the finite difference method for the fluid flow problem and the finite element method for the geomechanical problem. Due to the reduced computing cost, explicit coupling (see

Fung *et al.*, 1992; Tortike and Farouq Ali, 1993; Koutsabeloulis and Hope, 1998; Settari and Walters, 1999) is often preferred to iterative coupling (see Settari and Mourits, 1994, 1998; Chin and Thomas, 1999). Note that when using the iteratively coupled method for reservoirs with high rock compressibility and low fluid compressibility, close attention must be paid to the stability of the method (Bévilion and Masson, 2000). The partially coupled approach relies on a reformulation of the stress-flow coupling such that a conventional stress analysis code (that can receive thermal and pressure loads) can be used in conjunction with a conventional reservoir simulator. Due to this principle, partial coupling benefits from the latest developments in physics and numerical techniques in both reservoir and mechanical simulators, and the development effort is focused on the interface code between simulators. Furthermore, partial coupling allows the use of different meshes and time steps for the reservoir and geomechanical simulation. In fact, larger stress time steps than reservoir steps can effectively reduce mechanical computation cost, which can be huge compared with reservoir computation cost.

In the **fully coupled** approach, Equations (2) and (3) are simultaneously solved in the same simulator. The discretization methods used can be either the finite difference method (see Osorio *et al.*, 1998; Stone *et al.*, 2000) or the finite element method (see Lewis and Schrefler, 1998; Gutierrez and Lewis, 1998; Koutsabeloulis and Hope 1998; Chin *et al.*, 1998). The fully coupled method offers internal consistency for the simultaneous resolution of Equations (2) and (3). However, in this approach, hydraulic and geomechanical mechanisms are often simplified in comparison with conventional commercial geomechanical and reservoir approaches. As a result, the fully coupled approach requires considerable development to bring fluid flow and geomechanical capabilities on a par with existing commercial simulators (Settari and Walters, 1999).

3 THERMO-HYDRO-MECHANICAL MODELING OF A COMPARTMENTALIZED LIMESTONE RESERVOIR

The study deals with a highly heterogeneous and compartmentalized limestone reservoir in the Middle East where rapid water breakthrough was observed at some producers after the beginning of water injection. In parallel to an extensive fracture characterization study, the thermo-hydro-mechanical behavior of the field was analyzed over a five-year production period. The aim was to ascertain whether thermal gradients and dynamic changes in the effective stress state can induce opening/closure of existing fracture sets and/or microfracture initiation and propagation that could affect conductivity of fracture sets and preferred water flood directionality.

In conventional reservoir engineering analyses, the permeability of the fractured reservoir is usually defined in a static manner whereas coherent actualization implies the knowledge of stress evolution during production. The thermo-hydro-mechanical behavior of the fractured reservoir was accordingly studied using a 3D stress dependent reservoir simulator.

3.1 3D Stress Dependent Reservoir Simulator

A 3D stress dependent reservoir simulator ATH2VIS was developed to assess the thermo-hydro-mechanical behavior of complex reservoirs. This simulator is based on the partial coupling methodology (see the previous section) between the IFP ATHOS™ reservoir simulator and the VISAGE™ system (VIPS Ltd., 2001). Explicit coupling and iterative coupling can be obtained with different time steps for the reservoir and geomechanical simulators. The coupling between the two simulators is based on user-defined coupling periods and associated meeting times (see Fig. 3). This methodology helps to simulate highly compartmentalized reservoirs with very complex reservoir and geomechanical characteristics.

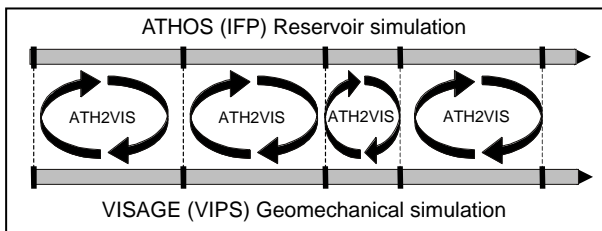


Figure 3
ATH2VIS partial coupling with different reservoir-geomechanical coupling periods.

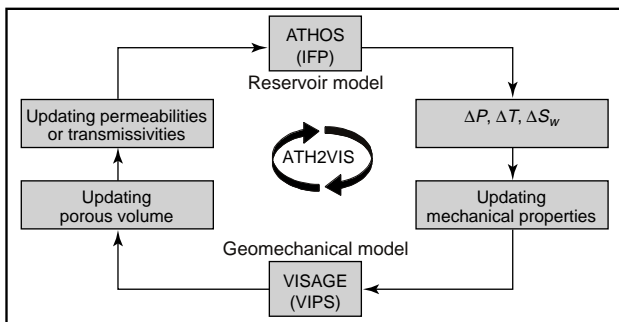
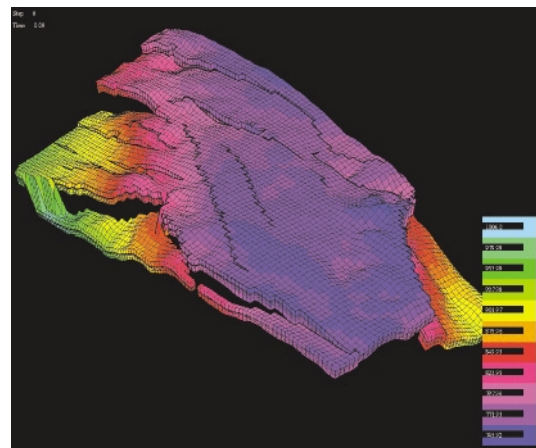
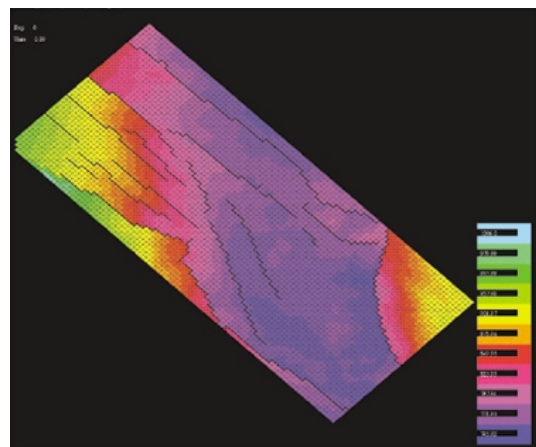


Figure 4
Data exchanges between reservoir and geomechanical model during an iteration.



(a)
Figure 5a
Reservoir geometry.



(b)
Figure 5b
Reservoir geometry in XY plane.

Figure 4 illustrates the exchanges between the reservoir and geomechanical simulators during a coupled analysis. The reservoir simulator computes pore pressure, saturation and temperature changes, and provides this information to the geomechanical simulator, which computes the evolution of stresses and strains induced by reservoir exploitation. In the case of a fractured reservoir, variations in stresses and strains given by the geomechanical computation in each grid cell are interpreted as permeability tensor variations (fracture permeability model) and used for an actualization of the permeability description in the reservoir model.

3.2 Thermo-Hydro-Mechanical Modeling of Reservoir Behavior During Production

The thermo-hydro-mechanical behavior of the reservoir during production is studied using the explicit partial coupling methodology. A specific analysis determines whether thermal gradients and dynamic changes in effective stress state can open or close existing fracture sets, induce fracturing and affect the conductivity of fracture sets and preferred water flood directionality.

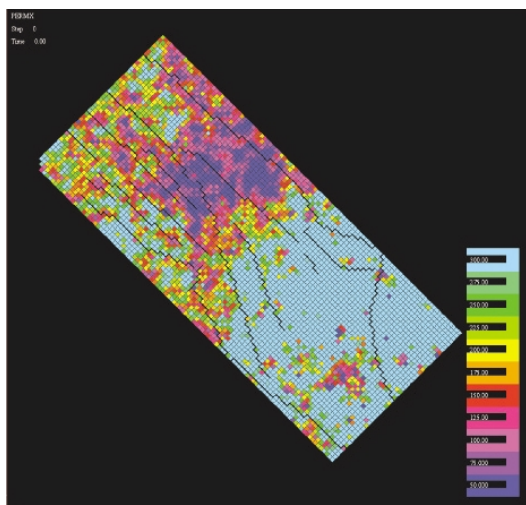


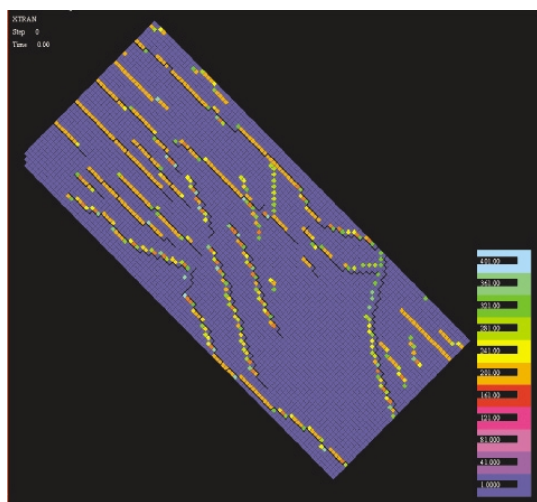
Figure 6
Permeability (x-direction) distribution in the reservoir (in mD).

3.2.1 Reservoir Model

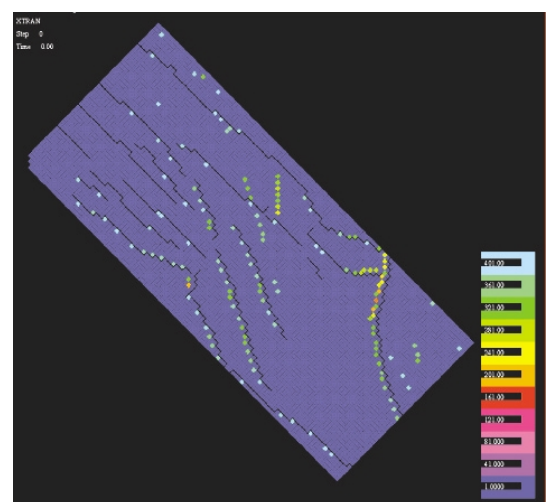
The field investigated was a highly heterogeneous and compartmentalized limestone reservoir located at 800 m depth. The reservoir geometry (Figs. 5a and 5b) was defined in corner point geometry and led to a total of 106*46*6 grid cells. The modeled reservoir included five producers and three water injectors. The reservoir initial temperature was 60°C. Water was injected at a bottom-hole temperature of 25°C. The reservoir model was based on single porosity description for fluid flows. For each grid cell, the homogenized grid cell permeability was defined using matrix and fracture permeability. The reservoir permeability distribution in the reservoir is given in Figure 6. In the reservoir model, the faults are described using directional transmissibility multipliers for the fluid flow problem (Figs. 7a and 7b).

3.2.2 Description of the Geomechanical Model

In the coupled ATH2VIS procedure, pore pressure and temperature variations calculated by the reservoir simulator are used in the geomechanical model as a loading for the stress and strain calculation. The geomechanical calculation requires modeling not only of the reservoir but also of its containment (over-, under- and side-burden), to apply boundary conditions and to define the thermo-hydro-mechanical properties of the intact rock, fracture and faults. The geometry of the geomechanical model including the reservoir and over-, under- and side-burden is shown in Figure 8. Figure 9 shows a local section of the model. In the geomechanical model, the faults act as mechanical interfaces



(a)



(b)

Figure 7
Transmissibility multipliers (Fault definition). (a) x-direction; (b) y-direction.

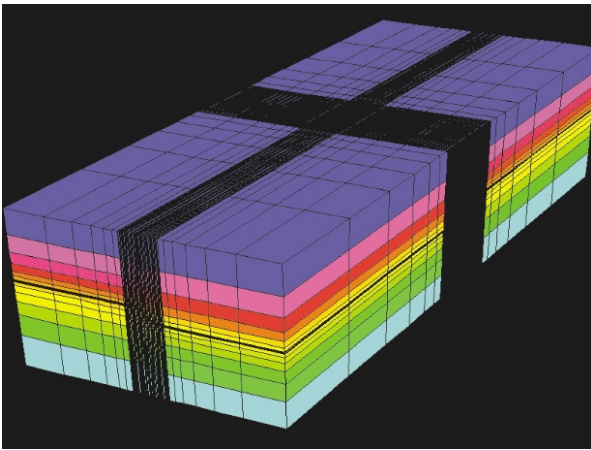


Figure 8
Geometry of the modeled structure including the reservoir.

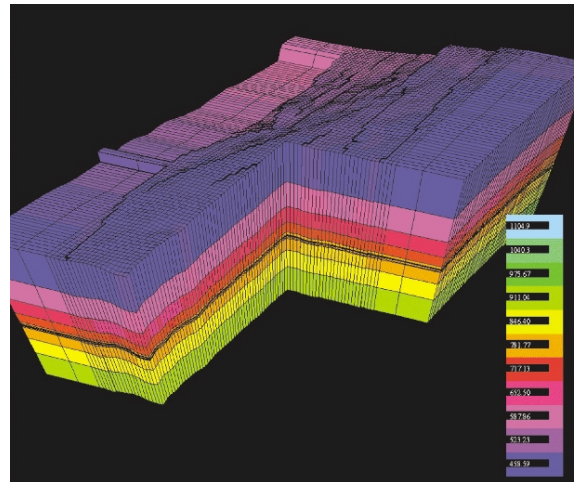


Figure 9
Geometry of a part of the modeled structure.

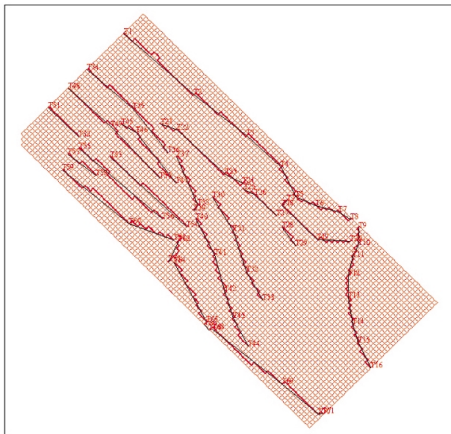


Figure 10
Mechanical description of faults.

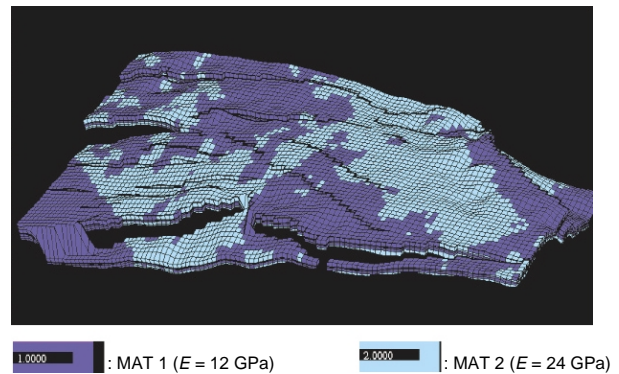


Figure 11
Material mechanical zonation.

where strain localization can occur due to stress perturbation induced by production. Figure 10 shows the faults that are incorporated in the geomechanical model.

An extensive laboratory study was conducted to determine the thermo-hydro-mechanical properties of the reservoir rock. Two mechanical rock types were defined with respect to dolomitic content. The distribution of the two mechanical rock types in the reservoir is given in Figure 11; low dolomitic content reservoir rock type is indicated in blue (indicator equal to 1, MAT1) and high dolomitic content reservoir rock type is indicated in white (indicator equal to 2, MAT2). The associated mechanical properties are given in Table 1.

The initial stress state (start of exploitation) was obtained by computing the mechanical equilibrium of the model subjected to regional stresses. The regional stresses are

defined by the gradients of the total vertical stress, maximum horizontal stress and minimum horizontal stress (Table 2). At 800 m depth, it leads to the following stress state:

- total vertical stress: $\sigma_v = 168$ bar;
- total max. horizontal stress: $\sigma_H = 160$ bar;
- total min. horizontal stress: $\sigma_h = 104$ bar.

Assuming a pore pressure of 88 bar at a depth of 800 m, total stresses are converted in terms of effective stress. Hence the effective stress state is given by:

- effective vertical stress: $\sigma'_v = 80$ bar;
- effective max. horizontal stress: $\sigma'_H = 72$ bar;
- effective min. horizontal stress: $\sigma'_h = 16$ bar.

The maximum horizontal stress makes an angle of 80° with north direction.

TABLE 1

Thermo-poro-mechanical properties of the reservoir rock

	MAT 1	MAT 2
Young's modulus (bar)	120 000	240 000
Poisson's ratio	0.2	0.2
Thermal expansion ($^{\circ}\text{C}^{-1}$)	$2.5 \cdot 10^{-5}$	$2.5 \cdot 10^{-5}$
Cohesion (bar)	40	113
Friction angle (deg)	34	34
Dilatation angle (deg)	5	5
Biot's coefficient	1	1

TABLE 2

Gradient of total and effective stresses (measured at reservoir depth)

Gradient of total and effective stresses	bar/m	psi/ft
Total vertical stress	0.21	1
Tot. max. horiz. stress	0.20	0.95
Tot. min. horiz. stress	0.13	0.63
Effective vertical stress	0.1	0.48
Eff. max. horiz. stress	0.09	0.43
Eff. min. horiz. stress	0.02	0.096

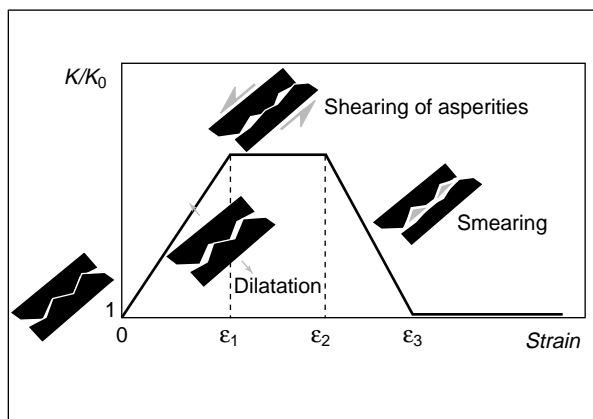


Figure 12

Description the fracture and fault permeability-strain model.

3.2.3 Permeability-Strain Model

The permeability strain model is used in the “updating permeability” step of the coupled methodology illustrated in Figure 4. This model (Koutsabeloulis and Hope, 1998) describes fracture and fault permeability evolution as a function of normal and shear strains on fault and fracture planes. This model can be presented in a conceptual way as indicated by Figure 12. Different physical mechanisms are considered, which contribute to increase or decrease the joint

permeability. The first mechanism is joint dilatation (deformation perpendicular to the joint plane) which tends to increase permeability in the direction of the joint plane. Once dilatation reaches a given magnitude, the shear strains that occur on the joint plane cause a smearing effect that reduces the joint permeability in the perpendicular direction to the joint plane.

3.2.4 Coupled Simulation

The thermo-hydro-mechanical behavior of the reservoir was analyzed over a five-year production period (1827 days). Water injection started 458 days after the start of production.

The partially coupled simulation was divided into two steps. A first mechanical computation (initialization) was performed to reach a mechanical equilibrium between the applied boundary conditions (regional stresses) and the initial state of stress in the reservoir. The partially coupled simulation was then performed using user-defined coupling periods (see Fig. 3):

- 0 days (initial mechanical equilibrium under regional stress state);
- 0-243 days;
- 243-943 days;
- 943-1522 days;
- 1522-1827 days.

During each coupling period, variations in pore pressure, temperature, strains and stresses were computed and an updated reservoir grid cell transmissibility determined using the fracture and fault permeability-strain model. The updated transmissibility field was integrated in the simulation of the next period (explicit coupling, see Fig. 4).

At the start of exploitation, oil production causes an overall pore pressure decrease in the field. The start of water injection, after 458 days of exploitation, offsets oil production and lead to pressure maintenance in the field. Maps of pore pressure distribution in the field are given in Figures 13a and 13b at the beginning and after 5 years of exploitation. We found that the reservoir exploitation (production and water injection) leads to a 5 bar depletion magnitude in the south part of the modeled sector after five years. Figures 14a and 14b show the evolution of water saturation at the beginning and after 5 years of exploitation. As water is injected at a bottom-hole temperature of 25°C in a reservoir rock at 60°C , cooling of the reservoir rock takes place. Maps of temperature distribution in the reservoir are given in Figure 15a for the uncoupled reservoir simulation and in Figure 15b for the coupled reservoir-geomechanics simulation. We found that cooling remains localized around the injectors and that the shape of the cooled area is more directional with coupled modeling than with conventional reservoir modeling. This is due to a thermal fracturing mechanism, represented by the coupled reservoir-geomechanical simulation, which causes a change in fluid flow directionality. The cooling of the

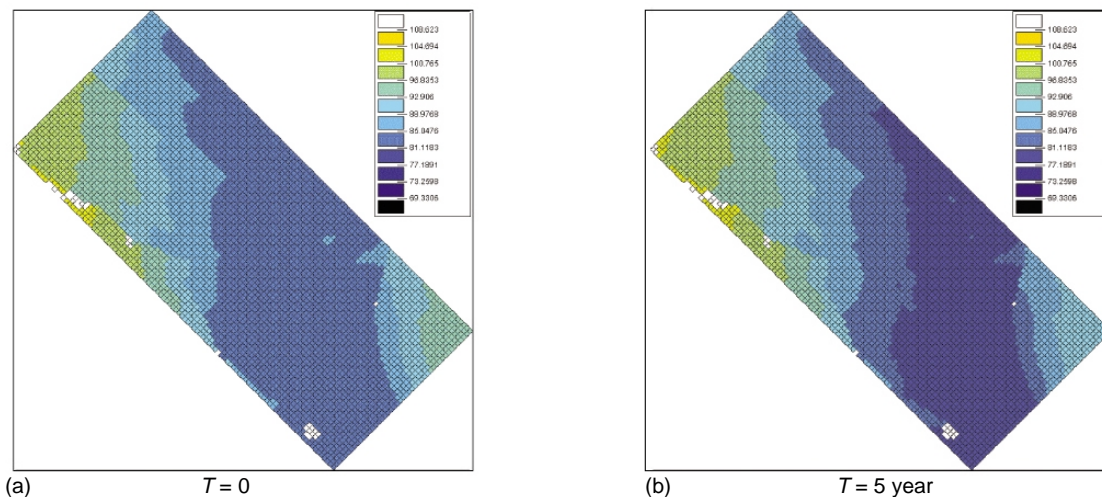


Figure 13

Pore pressure (bar) (coupled simulation). (a) $T = 0$; (b) $T = 5$ years.

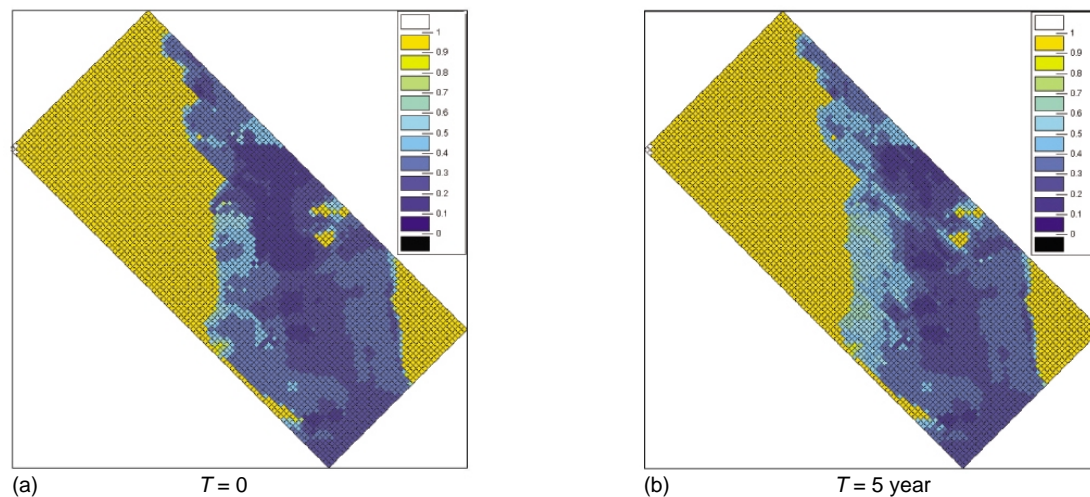


Figure 14

Water saturation (coupled simulation). (a) $T = 0$; (b) $T = 5$ years.

reservoir rock around the injector causes the in situ stress to drop below the injection pressure then leading, to a preferred flooding direction perpendicular to the local minimum horizontal *in situ* stress.

At reservoir scale, Figure 16 shows that the modification of the reservoir stress equilibrium, caused by changes in pore pressure and temperature during exploitation, gives rise to substantial strain localization on some faults. More specifically, only specific parts of the faults are critically stressed depending on pore pressure and temperature variations and fault strikes compared with the maximum in situ compressive stress direction. In the partially coupled analysis, these normal strains on faults are interpreted in terms of permeability variations using the fracture and fault permeability model previously presented. The fault

permeability multipliers calculated in the x - and y - directions are shown in Figures 17a and 17b.

In conclusion, the analysis presented shows how reservoir exploitation can modify the stress equilibrium of a reservoir and result in strain localization on some faults and fractures. The results presented show how geomechanical effects can contribute in modifying the reservoir properties. In the case study, the results obtained indicate that only specific parts of the faults are critically stressed. The mobilization of faults depends on their strike with respect to the maximum horizontal compressive stress direction, their location, the reservoir characteristics (mechanical properties and geometry) and exploitation conditions (local magnitude of pressure and temperature gradients determined by the location of injectors and producers, and magnitude of flow rates).

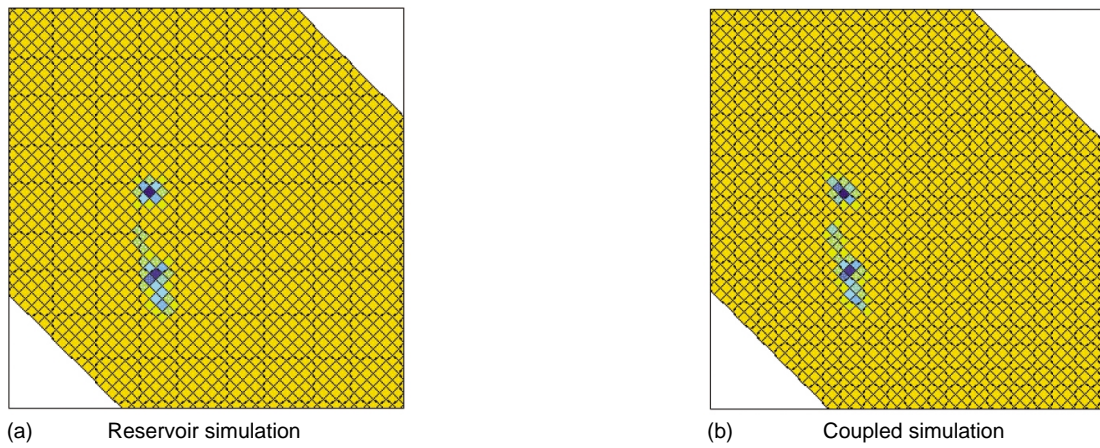


Figure 15
Temperature maps ($T = 5$ years). (a) reservoir simulation; (b) coupled simulation.

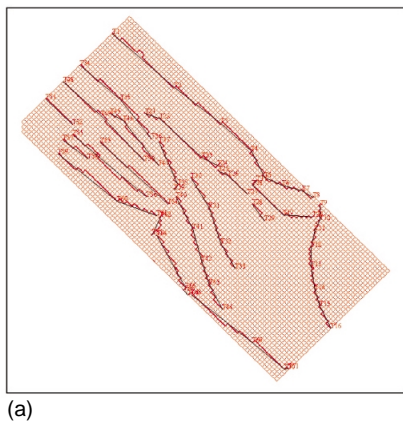


Figure 16a
Fault distribution in the reservoir.

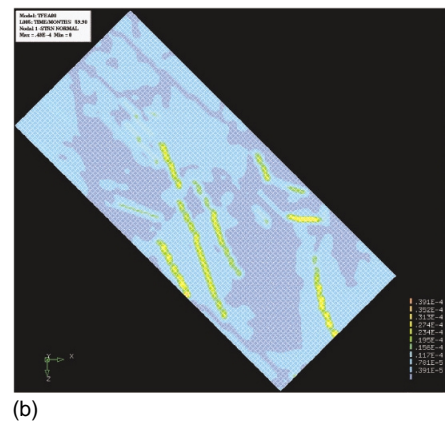


Figure 16b
Maps of normal strains on faults.

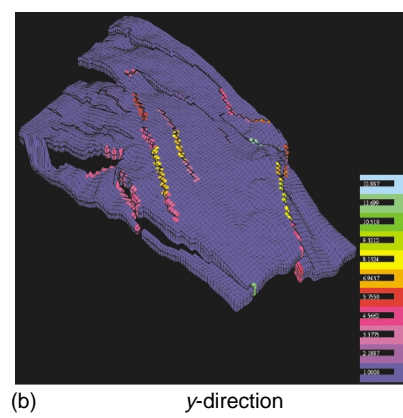
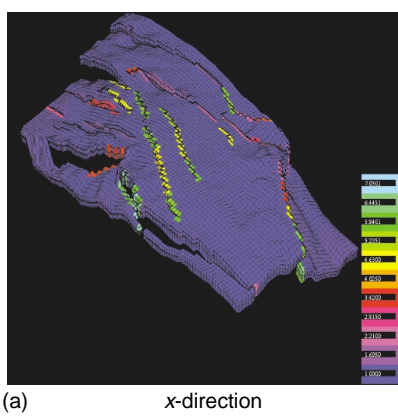


Figure 17
Fault transmissibility multipliers. (a) x-direction; (b) y-direction.

CONCLUSIONS

During reservoir production, space-time variations in reservoir pressure, saturation and temperature can modify the reservoir stress equilibrium with highly pronounced geomechanical effects depending on reservoir properties (poorly compacted reservoirs, fractured and faulted reservoirs). The main mechanisms and constitutive behaviors associated with the production of stress sensitive reservoirs have been described such as, compaction drive for weakly compacted reservoirs and thermal fracturing for highly compacted reservoirs. These geomechanical effects can be accounted for by a highly developed geomechanical analysis that must include non linear elasto-plastic constitutive behavior, fracture mechanics, water weakening effects, stress path and initial stress state influences. Different methodologies (fully coupled, partially coupled, one-way coupled) usable to solve a coupled thermo-hydro-mechanical problem with stress dependent reservoir simulators are discussed. The fully coupled approach simultaneously solves the whole set of equations in one simulator. It yields to consistent descriptions but published works indicate that the hydraulic or geomechanical mechanisms are often simplified in comparison with conventional uncoupled geomechanical and reservoir approaches. The partially coupled approach is based on an external coupling between conventional reservoir and geomechanical simulators. This approach has the advantage of being flexible and benefits from the latest developments in physics and numerical techniques of both simulators.

The application part presents a 3D partially coupled modeling between the ATHOS reservoir simulator and the VISAGE™ system (VIPS Limited, 2001). The aim of this study was to quantify geomechanical effects associated with reservoir exploitation, particularly thermal fracturing and fault and fracture permeability enhancement. The reservoir model represents a highly heterogeneous and compartmentalized limestone reservoir. The results presented indicate that during reservoir exploitation, changes in pore pressure and temperature give rise to a modification of the reservoir stress equilibrium and to progressive strain localization on some faults. Only specific parts of these faults are critically stressed depending on pore pressure and temperature variations and fault strikes compared with maximum compressive stress direction. Using a fracture and fault permeability model, the progressive straining of faults is interpreted in terms of permeability enhancement in the partially coupled analysis.

ACKNOWLEDGEMENTS

The authors thank *TotalFinaElf*, *IFP*, *Beicip-Franlab* and *VIPS Ltd.* for permission to publish this paper, and gratefully acknowledge the support of *TotalFinaElf* for the field case study.

REFERENCES

- Bévilion, D. and Masson, R. (2000) Stability and Convergence Analysis of Partially Coupled Schemes for Geomechanical-Reservoir Simulations. *7th European Conference on the Mathematics of Oil Recovery, ECMOR*, Baveno, Sep. 5-8.
- Biot, M.A. (1941) General Theory of Three-Dimensional Consolidation. *Journal of Applied Physics*, **12**, 155-164.
- Boutéca, M. (1992) Elements of Poro-Elasticity for Reservoir Engineering. *Revue de l'Institut français du pétrole*, **47**, 4, 479-490.
- Boutéca, M.J., Sarda, J-P. and Schneider, F. (1996). Subsidence Induced by the Production of Fluids. *Revue de l'Institut français du pétrole*, **51**, 3, 365-379.
- Charlez, P.A. (1997). *Rock Mechanics, Petroleum Applications*, **2**, Éditions Technip, Paris, France.
- Chin, L.Y., Raghavan, R. and Thomas, L.K. (1998) Fully-Coupled Geomechanics and Fluid-Flow Analysis of Wells with Stress-Dependent Permeability. *SPE International Conference and Exhibition*, Beijing, China, 2-6 Nov., 269-284
- Chin, L.Y. and Thomas, L.K. (1999) Fully Coupled Analysis of Improved Oil Recovery by Reservoir Compaction. *SPE Annual Technical Conference and Exhibition*, Houston, Texas, 3-6 October. 393-401
- Coussy, O. (1995) *Mechanics of Porous Continua*, Wiley, New York.
- Ferféra, F., Sarda, J.-P., Boutéca, M., and Vincké, O. (1997) Experimental Study of Monophasic Permeability Changes under Various Stress Paths. *International Journal of Rock Mechanics and Mining Sciences and Geomechanics*, **34**, 3-4, 1997, Paper no. 037.
- Fung, L. S. K., Buchanan, L. and Wan, R. G. (1992) Coupled Geomechanical-Thermal Simulation for Deforming Heavy-oil Reservoirs. *CIM Annual Technical Conference*, Calgary, June 7-10.
- Geertsma, J. (1989). On the Alert for Subsidence. *AGIP Review*, **6**, 39-43.
- Gutierrez, M. and Lewis, M. (1998) The Role of Geomechanics in Reservoir Simulation. *SPE/ISRM Eurock'98*, Trondheim, Norway, 8-10 July 1998, 439-448.
- Gutierrez, M. and Makurat, A. (1997) Coupled HTM Modelling of Cold Water Injection in Fractured Hydrocarbon reservoirs. *Int. J. Rock Mech. & Min. Sci.* **34**, 3-4, Paper no. 113.
- Heffer, K.J., Last, N.C., Koutsabeloulis, N.C., Chan, H.C.M., Gutierrez, M. and Makurat, A. (1994). The Influence of Natural Fractures, Faults and Earth Stresses on Reservoir Performance - Geomechanical Analysis by Numerical Modelling. *North Sea Oil and Gas Reservoirs - III*, 201-211, Kluwer Academic Publishers.
- Hermansen, H., Landa, G.H., Sylte, J.E. and Thomas L.K. (2000) Experiences after 10 years of Waterflooding the Ekofisk Field, Norway. *Journal of Petroleum Science and Engineering*, **26**, 11-18
- Homand, S. (2000) Comportement mécanique d'une craie très poreuse avec prise en compte de l'effet de l'eau : de l'expérience à la simulation. *Thèse de l'université de Lille*.
- Koutsabeloulis, N.C., Heffer, K.J., and Wong, S. (1994) Numerical geomechanics in reservoir engineering. *Computer Methods and Advances in Geomechanics*, Siriwardane and Zaman eds., Balkema, Rotterdam.
- Koutsabeloulis, N.C. and Hope, S.A. (1998) Coupled Stress/Fluid/Thermal Multi-Phase Reservoir Simulation Studies Incorporating Rock Mechanics. *SPE/ISRM Eurock'98*, Trondheim, Norway, 8-10 July 1998, 449-454.

- Lewis, R.W. and Schrefler, B.A. (1998) *The Finite Element Method in the Static and Dynamic Deformation and Consolidation of Porous Media*, Second Edition, Wiley, New York.
- Matà, C. (2001) Étude expérimentale et modélisation mécanique des effets du balayage à l'eau dans une craie saturée d'huile. *PhD Thesis* (in French), ENPC.
- Merle, H.A., Kentie, C.J.P., van Opstal, G.H.C. and Schneider, G.M.G. (1976). The Bachaquero Study - A Composite Analysis of the Behavior of a Compaction Drive/Solution Gas Drive Reservoir. *SPE JPT* September, 1107-1115.
- Osorio, J.G., Chen, H.Y., Teufel, L. and Schaffer, S. (1998) A Two-Domain, Fully Coupled Fluid-Flow/Geomechanical Simulation Model for Reservoirs with Stress-Sensitive Mechanical and Fluid-Flow Properties. *SPE/ISRM Eurock'98*, Trondheim, Norway, 8-10 July 1998, 455-464.
- Settari, A. and Mourits, F.M. (1994) Coupling of geomechanics and Reservoir Simulation Models. *Computer Methods and Advances in Geomechanics*, 2151-2158.
- Settari, A. and Mourits, F.M. (1998) A Coupled Reservoir and Geomechanical Simulation System. *SPE Journal*, 219-226.
- Settari, A. and Walters, D.A. (1999) Advances in Coupled Geomechanical and Reservoir Modeling With Applications to Reservoir Compaction. *SPE Reservoir Simulation Symposium*, Houston, Texas, 14-17 February.
- Stone, T., Garfield, B. and Papanastasiou, P. (2000) Fully Coupled Geomechanics in a Commercial Reservoir Simulator. *SPE European Petroleum Conference*, Paris, France, 24-25 October, 45-52.
- Tortike, W.S. and Farouq Ali, S.M. (1993) Reservoir Simulation Integrated with Geomechanics. *The Journal of Canadian Petroleum Technology*, **32**, 5, 28-37.
- VIPS Limited (2001). *VISAGE User's Guide, Version 7.6*. VIPS (Vector International Processing Systems) Limited, Elm Lodge, North Street, Winkfield, Windsor, Berkshire SL4 4TE, UK.
- Wong, T.F., David, C. and Zhu, W. (1997) The Transition from Brittle to Cataclastic Flow: Mechanical Deformation. *Journal of Geophysical Research*, **102**, B2, 10, 309-3025.

Final manuscript received in July 2002